Figure S1. Mouse *Bmncr* transcript sequence

AGGGTTCTGTGTTTTTTGTGGACACAGGTATATCTGCATGTGTATACTCAGCCTGGAAAAGACATAAAGGGCTTCTAATAGATGAATATAGGG
AAGGCAGATGGCCTCTGTCCTAGAAACTTAATCAGCAAGCCACAGAGGCTGTTTTCGGAACTCCCTGTGGGGTTTGGCTCAGCTAAGCGAA
CTC GGGAGCCAAGTTTGGCAGTAGAGGATGAAGAGAACTAAATTGCTCCACCTAAGAAATGAGAGGAATTTGGATTTTATCCCTAAGAGAG
ACATGGAGGAGACGGGGAAAGGCTTTCTGAATAATATGAACCAAAGCTCCATCCATCAATCCTGCTGTGCCCCATGAAGACTTTAACCCTTA
GAATAAGAATTGCCTGCCCCATTTCTACAAAATGAGTGTGTTCTTTGAGCAGAAGAGGAGAGAAGAGAAGAAATGGAACAATCTTTGCTTTG
GAAATTTAGCTGACTGGCCTCATTTGGAATAAGAGCGCCTTCAATCCCTGGCCGCAGGCGGGCAGTGGAGCCAACAGTAACACCGGATGC
TGGGATGCTGGGAGGAGGTCTGGAAGCATCAGAGGAGATGCCAGGGAACTTGGAGTCCAGAAGGCGGTAGTGGGTTCCTCTCTGGGGAT
GAGTCCCAGTTTCCTCAACTTTGTCCAGACCCCTTGTCCTCAGGCTAAAACCTACTATTTATTGGATAGAGCATTATCCTGGAAGCACTAAGA
GATTGGAGGAGAAGGTCCTGAGAAGAGCCAGAGGCCGGGTCTGCTTTGTGTCCTCGGCACCTACTTTCAGTCCATGACACATGAAAAGAG
CTGGAGTCAGAAGGACCAGGTGACTCAGGGGTGAGGCTTGAACTGCTTATGGAGCTGACCCACTACAGACTGGTGCCATCTGTGATGGAA
TGTTAAGAAAGGGAGTTGGTAGAATGAATCCTTCTCTTTAGCAAAAACGTTTCCTGCTCTGGCAATGCTGCGTTACAACGGCTGGAGGCCGC
TCTCCATAGAGACATCTCCTCGGGGCAGTTCACAACCCAGCAGCCTGCCTTACCCAGAGGAGAATCTGCCGACAGAGGAGAATCTATAGCA
GAATAGAAGACAGTCTGATGTGGCACAACGTAGAGGTGATATCCCAGCACCTGTGCTATACAGTGTTCTGCGGATGGGAAGCATGTCAAGG
GTCCTGCCCGTACAAGGTAGCACTCCAGGACACAGACAGCTAAAGATGGGAACGCCTGGGCTCCATTTCACAGTTTGTCTGCCACAGGTAA
TCCGTCAGAGGAGGAGAAGAACTAGATGGACAGGCCATAGAATCCACACTGGGTTAGGAAGGCTGTGGATATCAAAGGCCCTGACAAGAG
TGAAGAATTGTGGGAATAAGTCCAGTTTTTCAGCAGCCACCGCAGACACCCCTAAAATGGAAGAAGCACGTACGTTAACATATCCATCCCCT
TCCTCGCCCCTGTACCTCTTCGCTCCTGTCATACTCAATGCACCCCATCACAAGGTGCCAGGGCTAGAAAACGAGACCTAAGTCTTGGCTC
AGGAGTTGTACCCCTGGGACCCCCACACCAGTTCCTGTGCCCTCTTCGTGTCTTCACTCTAAACCGCCGCTCTCTGAATTTTGTACTTGTGG
TAAATCCCATCAATTGTTCGGACACTTGGGCACCAGGGATGGATGTACAGCCTCAGTCAGGGAAAATGGTTTCTTTCTCATGTCAGAATGCT
TTCTATGAGACTTTCTGTGAGACCTAAAGTGCCCGCTCCTTCTGATGAGGTCCGGGGAATCACGGGGAACCAGGGCACACAGGTTCTCTCT
CATATGCTCCAGCCAAAATAGTGAAAAAGGCCTTCCTGAGAGGAGAAGGTCTTACATGATGAAGCTGGACGCTGTGCAGCTATTTTTGATGC
CACCAACTGAAGCATGCACCACGAGGTTCCTGACAAGGGAACGGCTGACCCGCAGGTCAAGCTGCTGTGGTCAAGCATTTGTGGTTGGTA
ATGGAAGACAAAACCACGCAGCATTTCTCCAGCCCTGCTCTCTGAGCAGGTGTCTCTTCTGCCCTCTGAACACAGGATCTCTGAGAAGCCA
AGCTCTCTGTAACCCTCCTTTGGTGATGTGGCCTTGGTGTTCGTTCTCTGAGCAGAGGACTGTGGCTGTGGAGCTCTGGAGTCAGTCCATA
CTGGCTCACAAAAGCCGACTGTTAAAGTTTCCAGAACTCTGTGAGCCGGTTGTTAAGGACATACATCATTTGAAATTAAATTACATAAACTAA
CCATTACCTCACACTCAAAACAAGGCCACCGACTGCTCAGAATTCATTTACCAGTTACTTATTTTGTATTTTCTGTGTACCTGTGCTCTTTAGG
GTTACGAGCCTAACAGCAAGGGCATGACATGGAGAGTCAGTCACCAAGGGTCTCATTCCCACTGAGATCCAGGGACTTCACTTTGGCAGAT
CCACACAGGCCGTAGAAGTCAGCACCTGCCCCATATTCTCTAGGAGCTGCATGATAAACACCCATGCATAGCTAGACTCCAGGGGCCTGGG
GGAGACCCATTAAGATGACCACACCCTCCAGAAACTGCTCCTTCCCGGCCCTGGATTTCCTATCTTTGTGCATTAAAAAAAAAAAAAAAA

Figure S2. Human *BMNCR* transcript sequence

ATGCTGAATAAATGTCTGCTGGGAGAATGCATGAATGAATGAATGCATGGAGGAAGAGGAAGGAGAGGAAGAGAGAAGAAGATAGTG
GGAAGGAAGAGAGGAAGAGGAAATAAAAAACAGGAAAAGGAGATGGAAGAAGAAGGAGAGTGCAGTATAGGGTCGGAAAGAAAAAAGG
CATCCCTTGATTTGATCTTATCCCCTTTGTCTTCCTGGGGACTGGAAGGCCCTTCTCAGTTCCTTTCTTTTCCCTCTCCTCCCAACAGGAT
AAGGACTTTGGCCACAGCCCTGCCTATCCCCCAGGTATCCCCATAAAGTCTTTAACCCTTAGATATAGAACTGCTCTGTCCCTTTTCTACA
AAACAAATGTGTTATTTGGGCAGAAGAGGAAAGGAGAAAATTTGAAGTGGAAAAATCTTTGGTTTGGAAATTCAGCTGACTGCCCTCATTT
GGAATAAAATGTCCTTCAGTCCCTGGCTGTGTGGCAGGCAGGCCCGGCCAACAGCAACACCGGATGCCGGGAGACTGGGAGGAGGCC
TGGGGATTTTCAGAGGAGCCGCCAGAGTGGTATGAACTTGGAATCCAGGAAGAGAGTGATGGGGCTCATCTCCAAGGGCTGAATCCCTA
TCCTCTTCCTCATCTCTGTCCAGACAGTGGTCAGTTGTCCCGATGTGTCAGGCAGAGTGCTGTCCTGGGGGCACAGACAGGACCAGGAG
AAGCAAGTCCTGAGGGAGAACAGGGGCTGGGTCTGTCTCATGTCCTGAGCACCAACCTCAGCATCTGACACATGGAAGGTACCCAAGAA
ACATCAGCTGGGAAAAAAAAAGTAACCCTTGTCCCGAGGGGTTGACAGGAGACCCAGACTTTGCACTCAGGAGAGAGGGAGGTTGGAA
GCGCCACTGAGAGGAGTCAGAGGAAAGTGTAAGGAGACTTGTAAAAAAAGGAGGTGGTCATGAGGATGAAAGTCATATGTGAAGGATGA
TGGAACAGAGGGACTAAAGGAGCCTGCCCTGGACACCCTGATTTCCTGCTATGGGGAGTGAAAAAGAAGCCATAGTCCCATGGATTCTG
TTACCAGCCACTGAGTGCAATCCTACCTGATCCCATGGTCCTCACCAAGGCTGTGTCTGCTTAGGAAATGGAGAATGGTCCCCAAACCAC
AGCAGCAAAAATGAGTGGAAGGGTTGAGCATTATTTCCAGCCTTGGTTGCTCTGGTGATTGGTGCCTGGGAGGGGCAGGACCTCCATCC
AACAGACTGTACCAGCAGAGTCGTAAGAGGTAGGACTTTGGAGATTCAGCCGTATGTTCTATGGGTGGACTGAAGGCTGAAGGAGGAAG
AGGTAGAAGTGCATTGCTACCGACCTACTCCATCCCACGTGCAGACTCCCTCGACCCCCAACCCCAGGCTGTCACCTGCTCCTATATTC
ATTTTCTCTGAGGTTGGAGGAAAGAGAAAGGAGACAGCAATGGCCAGACTTCCCTGGGGTTCCCAAACTGGTTACTGTGCTCTGCTCAA
GTGCTGGCTCCCCGCCCCTCTCTATGCACACACTCAGCCCATGTTCACTGATTCCCATCCTACCCTCCAGTCATTTGCCTAACTGACTTT
TTTTTTTCCAGGAAACCTCAGAGATGCATTGGACTTGGTCAGCAGACTTGAGTTCTATGCCCATGCCAGTCACTGACTGGCCATGACCTG
AGTTGGACAAATCATGCCCACTCTAGACTTAAGTTGTTCCTTATATGGAAAAGGAAAGGAGTGCTTTGTCAGTGGTTCCCAGATACCAATT
TATAAAGATTTCACTAGTCTGTGGCAAAATAATATAACAATGGCTATGAATTACTGGGTATTTCCTTTGTGTGAAGTGGTTTTCATATATTAA
CTCATTTAATCTCATAACCACCTGGAAAAGTATGTATTCTTATTAACACCTTCACATGATAGATGATAAAACCAAGGCTCAGAGAGGTTAAG
TAACTTACCTGAAGGTCTTCATATGGTAAGTGGTAGAGCCTGGATTTGAACTCAGGTATCCTGGTCCCAGAGTCCACGTACTAAATCACTA
CATTACAGCTACCCATGTGATAAGGAAAAAGTAAGG

Figure S3

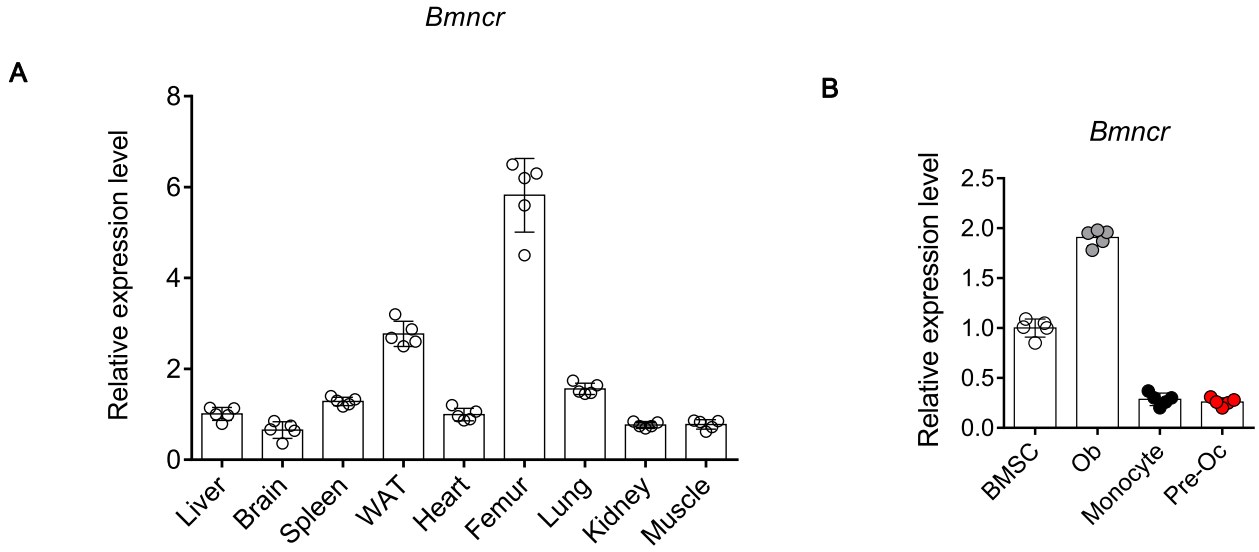

Figure S3. *Bmncr* expression pattern in mice.

(**A**) QRT-PCR analysis of the levels of *Bmncr* expression in different tissue in mice.

(**B**) QRT-PCR analysis of the levels of *Bmncr* expression in BMSCs, osteoblasts, monocytes and preosteoclasts from mice. n = 5 per group. Data shown as mean ± s.d.

Figure S4

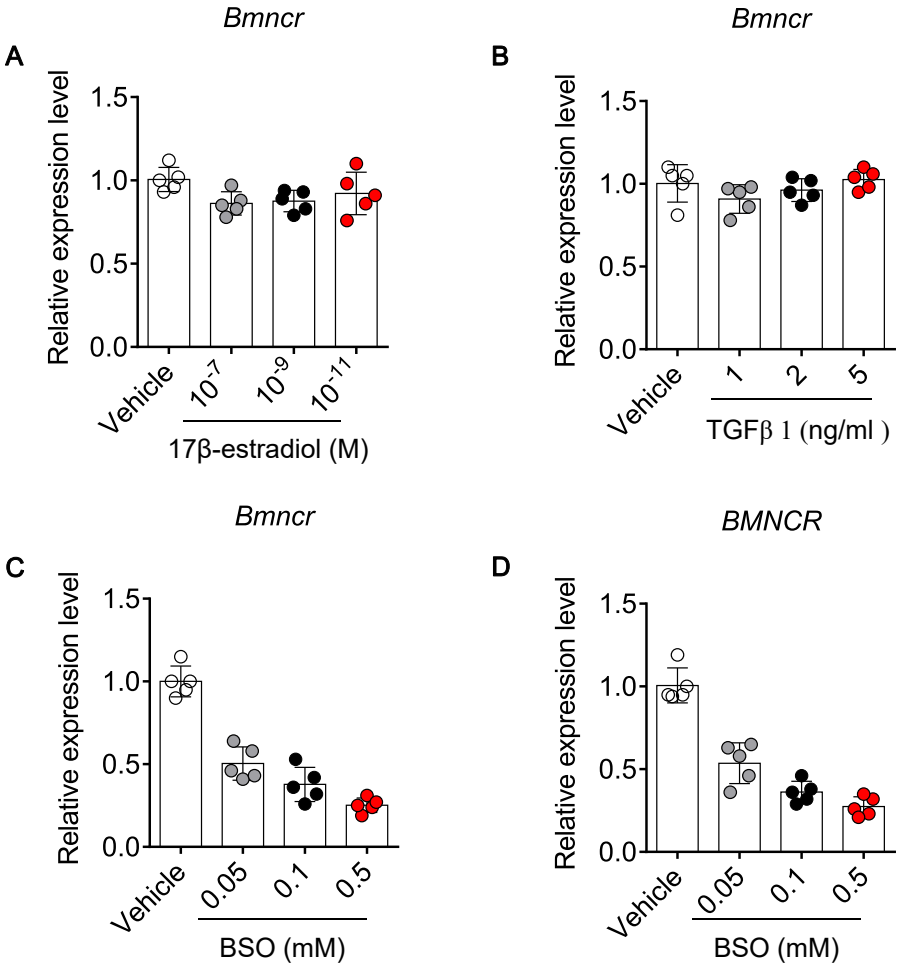

Figure S4. The influence of 17β-estradiol, TGF-β1 and BSO in *Bmncr* expression.

(**A-C**) QRT-PCR analysis of the levels of *Bmncr* expression in mice BMSCs with the administration of 17β-estradiol, TGF-β1 and BSO.

(**D**) QRT-PCR analysis of the levels of *BMNCR* expression in human BMSCs with the administration of BSO .

n = 5 per group. Data shown as mean ± s.d.

Figure S5

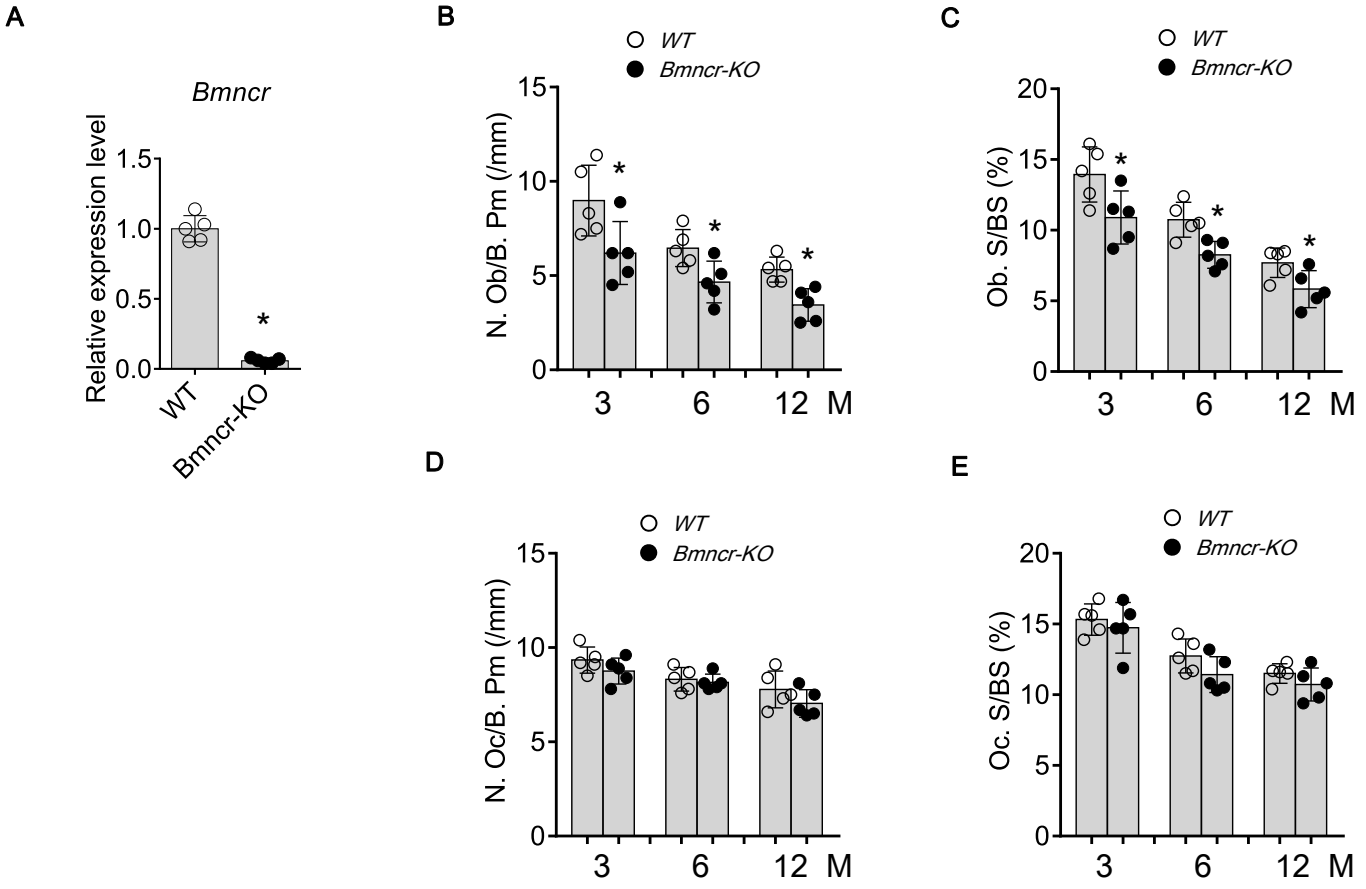

Figure S5. Histomorphometric analysis of femur in *Bmncr-KO* mice.

(**A**) QRT-PCR analysis of the levels of *Bmncr* expression in BMSCs derived from *WT* and *Bmncr-KO* mice. Number (**B**) and surface (**C**) of osteoblasts normalized to trabecular bone surface in femur. Number (**D**) and surface (**E**) of osteoclasts normalized to trabecular bone surface in femur. n = 5 per group. Data shown as mean ± s.d. *$P < 0.05$ (Student's *t*-test).

Figure S6

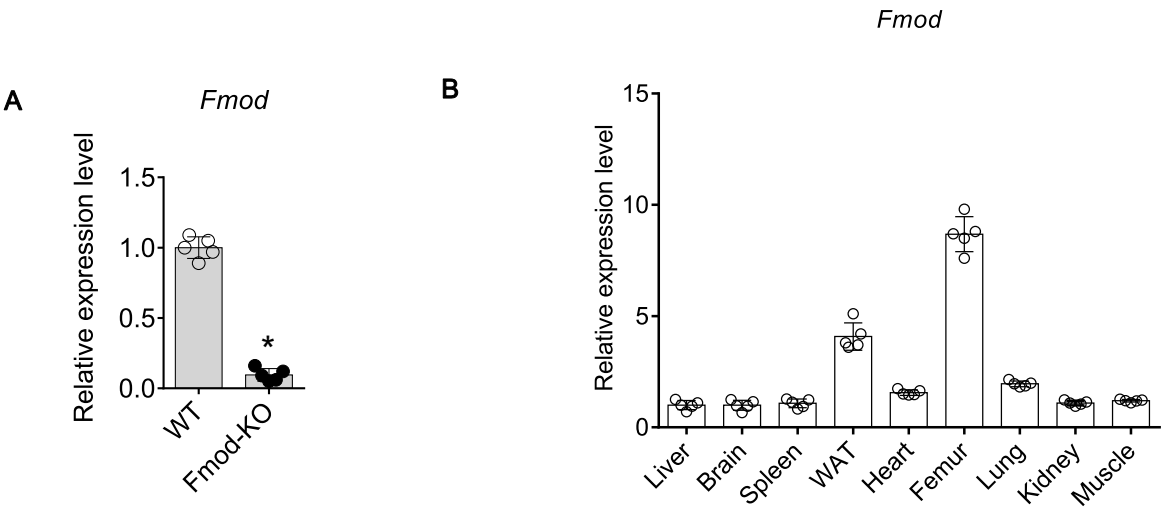

Figure S6. *Fmod* expression in *WT* and *Fmod-KO* mice.

(**A**) QRT-PCR analysis of the levels of *Fmod* expression in BMSCs derived from *WT* and *Fmod-KO* mice.

(**B**) QRT-PCR analysis of the levels of *Fmod* expression in different tissue from *WT* mice.

n = 5 per group. Data shown as mean ± s.d. *$P < 0.01$ (Student's *t*-test).

Figure S7

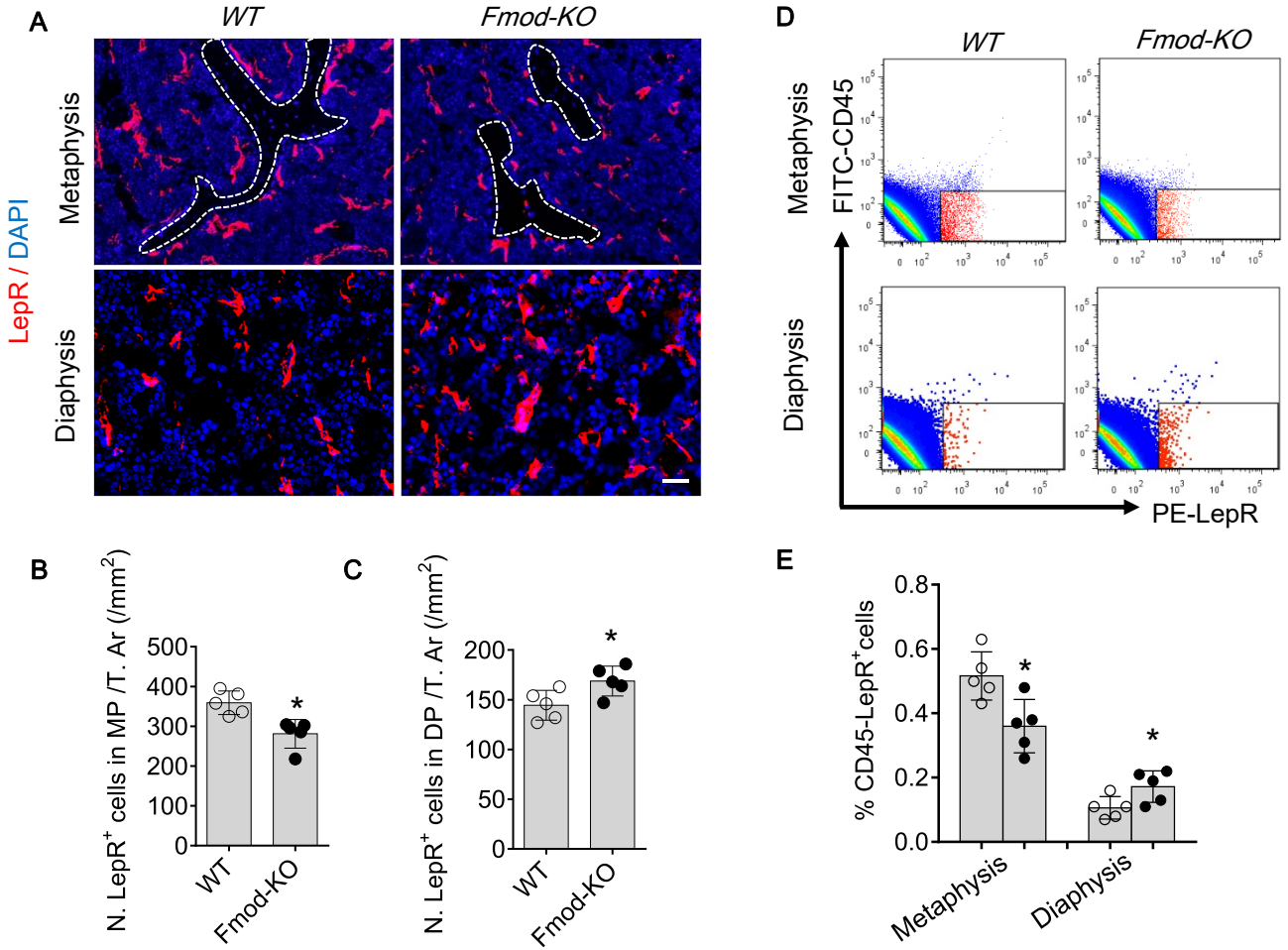

Figure S7. *Fmod-KO* mice exhibited reduced adherent ability of BMSCs to bone surface.

(**A**) Representative immunofluorescence staining images of leptin receptor (LepR) (red) in femora from wild-type (*WT*) and *Fmod null* (*Fmod-KO*) mice. Nuclei, DAPI (blue). Scale bar: 100 μM. (**B-C**) Quantitative analysis of the number of $LepR^+$ BMSCs in metaphysis (MP) and diaphysis (DP) region of femora. n = 5 per group. (**D-E**) FACS analysis dot plot (**D**) and quantitation of $LepR^+$ BMSCs (**E**) from *WT* and *Fmod-KO* mice. n = 5 per group. Data shown as mean ± s.d. **P* < 0.05 (Student's *t*-test).

Figure S8

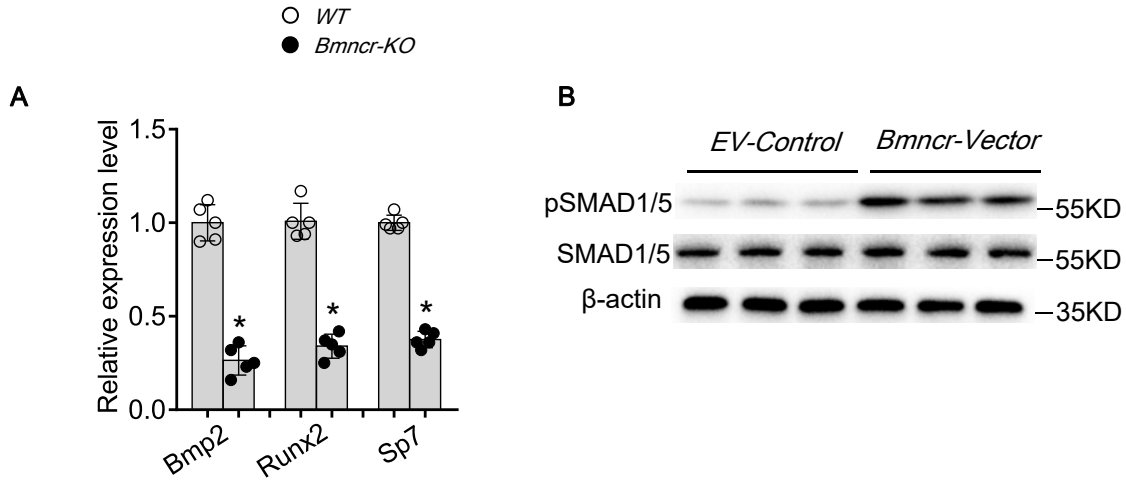

Figure S8. *Bmncr* regulated osteogenic gene expression and BMP2 signaling pathway in BMSCs.

(**A**) QRT-PCR analysis of the levels of *Bmp2, Runx2* and *Sp7* expression in BMSCs derived from *WT* and *Bmncr-KO* mice. (**B**) Western blot analysis of the pSMAD1/5 and SMAD1/5 protein level. β-actin was used as loading control. Data are representative of 3 independent experiments. n = 5 per group. Data shown as mean ± s.d. **P* < 0.01 (Student's *t*-test).

Figure S9

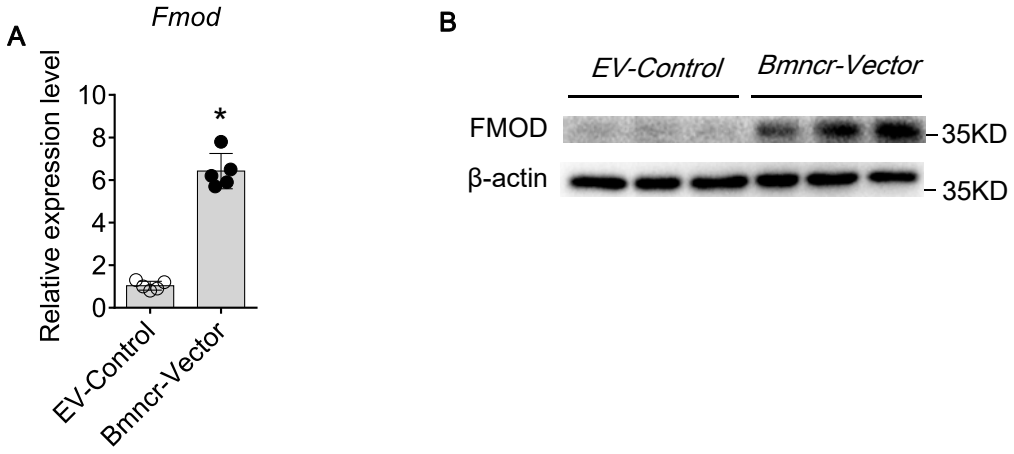

Figure S9. *Bmncr* regulated *Fmod* gene expression and protein in BMSCs.

(**A**) QRT-PCR analysis of the levels of *Fmod* expression. (**B**) Western blot analysis of the FMOD protein level. β-actin was used as loading control. Data are representative of 3 independent experiments. n = 5 per group. Data shown as mean ± s.d. **P* < 0.01 (Student's *t*-test).

Figure S10

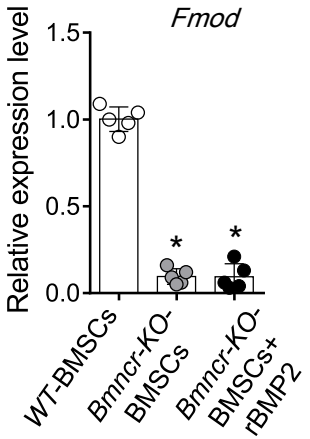

Figure S10. BMP2 didn't mediate the effects of *Bmncr* on *Fmod* gene expression in BMSCs.

QRT-PCR analysis of the levels of *Fmod* expression in BMSCs in indicated groups. n = 5 per group. Data shown as mean ± s.d. *$P < 0.01$ (one-way ANOVA)

Figure S11

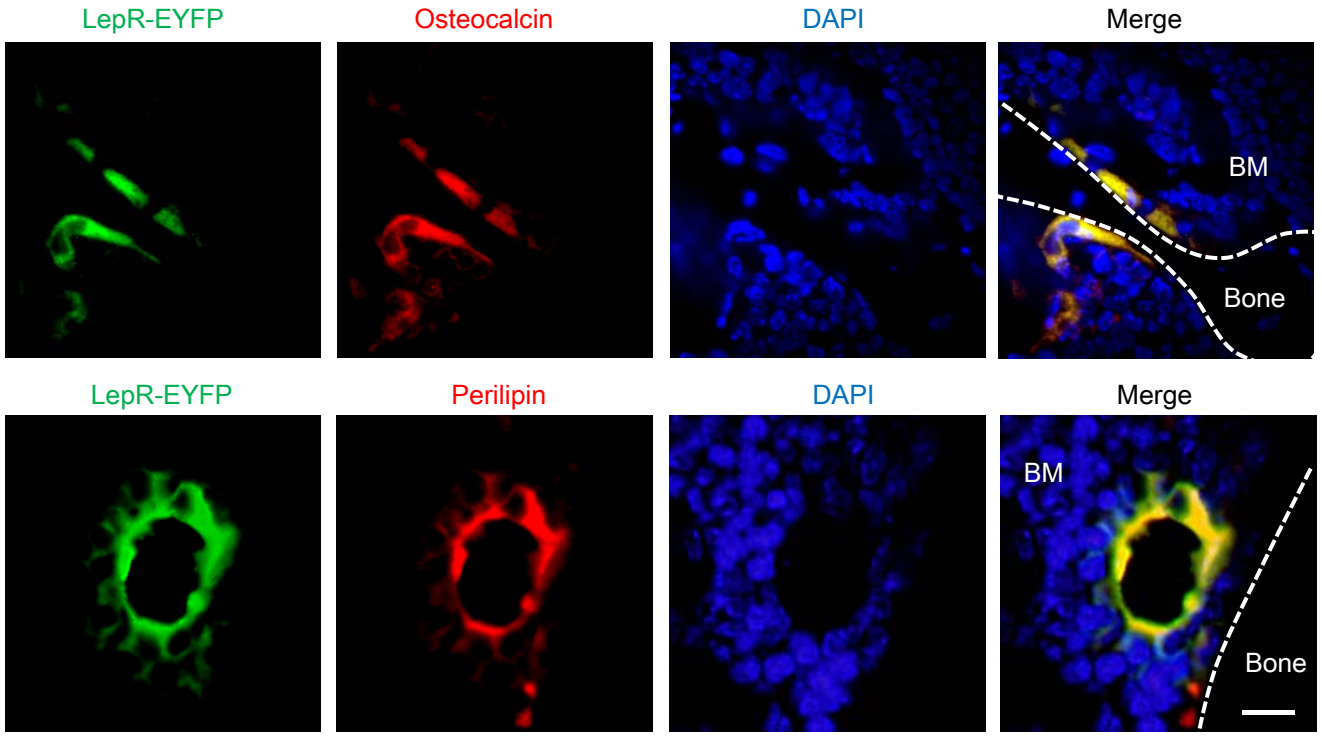

Figure S11. Leptin receptor expressing cells represent the progenitors of osteoblasts and adipocytes.

Representative immunofluorescence staining images of LepR-EYFP (green) with osteocalcin (red) or perilipin (red) in femora from *LepR-Cre;Rosa26-EYFP* $^{flox/flox}$ mice. Nuclei, DAPI (blue). Scale bar: 50 μM.

Figure S12

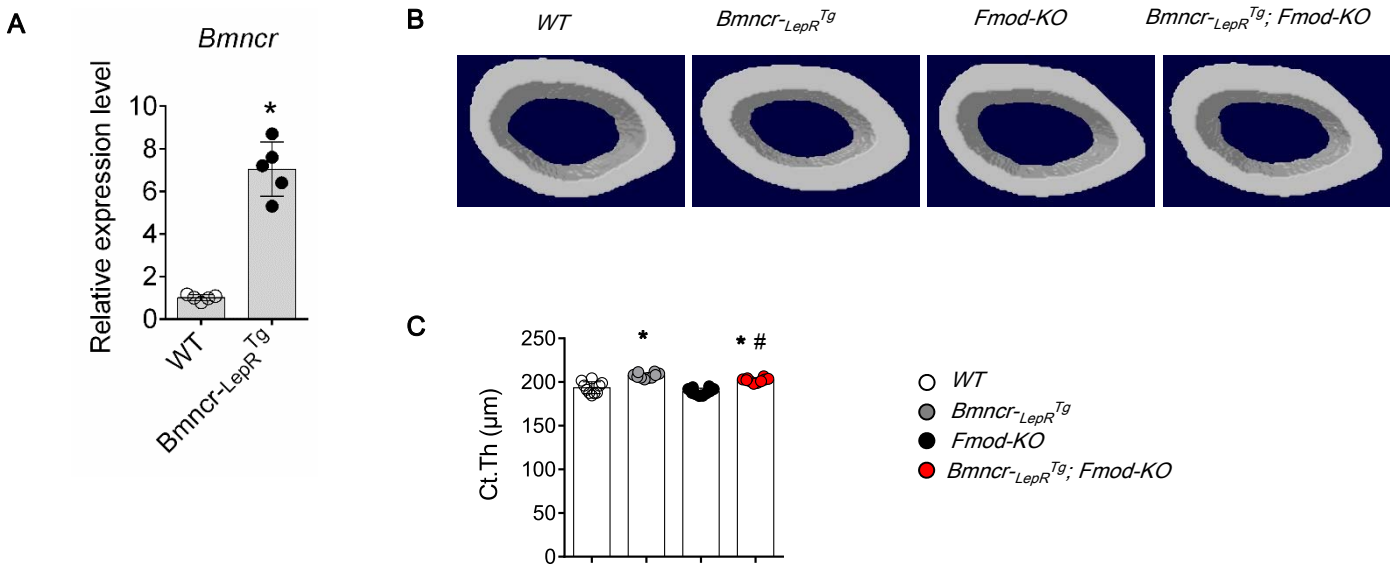

Figure S12. *Bmncr-*$_{LepR}^{Tg}$ mice showed increased cortical bone thickness in the femora compared to *WT* controls. (**A**) QRT-PCR analysis of the levels of *Bmncr* expression in BMSCs derived from *WT* and *Bmncr-*$_{LepR}^{Tg}$ mice. n = 5 per group. *P < 0.05. (Student's *t*-test). (**B-C**) μCT images (**B**) and quantitative μCT analysis (**C**) of cortical bone thickness in femora. n = 10 per group. *P < 0.05 versus WT group; # P < 0.05 versus Bmncr-$_{LepR}^{Tg}$ group (one-way ANOVA).

Figure S13

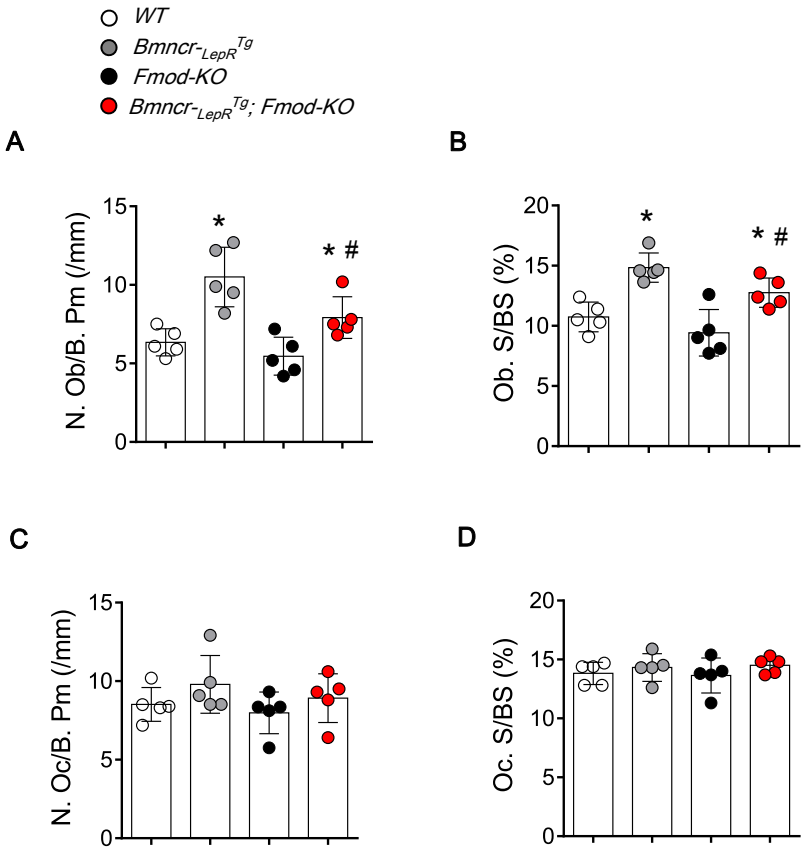

Figure S13. Osteoclastic bone resorption was not affected in *Bmncr-$_{LepR}^{Tg}$* mice.

Number (**A**) and surface (**B**) of osteoblasts normalized to trabecular bone surface in femur. Number (**C**) and surface (**D**) of osteoclasts normalized to trabecular bone surface in femur. Data shown as mean ± s.d. *P < 0.05 versus *WT* group; # P < 0.05 versus *Bmncr-$_{LepR}^{Tg}$* group (one-way ANOVA).

Figure S14

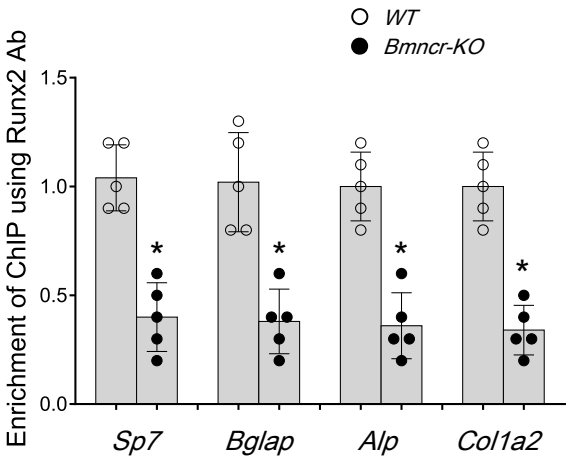

Figure S14. *Bmncr* regulated RUNX2 activities on target genes.

ChIP-PCR analysis of the levels of *Sp7, Bglap, Alp and Col1a2* expression using RUNX2 antibody in BMSCs derived from *WT* and *Bmncr-KO* mice. n = 5 per group. Data shown as mean ± s.d. **P* < 0.01 (Student's *t*-test).

Figure S15

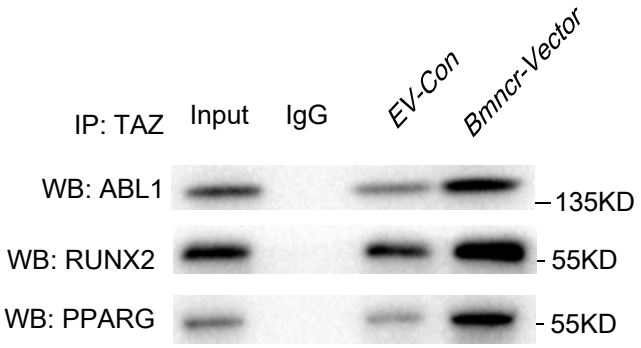

Figure S15. *Bmncr* regulated ABL-TAZ and TAZ-RUNX2/PPARG complex.

Immunoprecipitation assays using antibody against TAZ, the TAZ-associated ABL, RUNX2 and PPARG was detected by western blotting. Data are representative of 3 independent experiments.

Figure S16

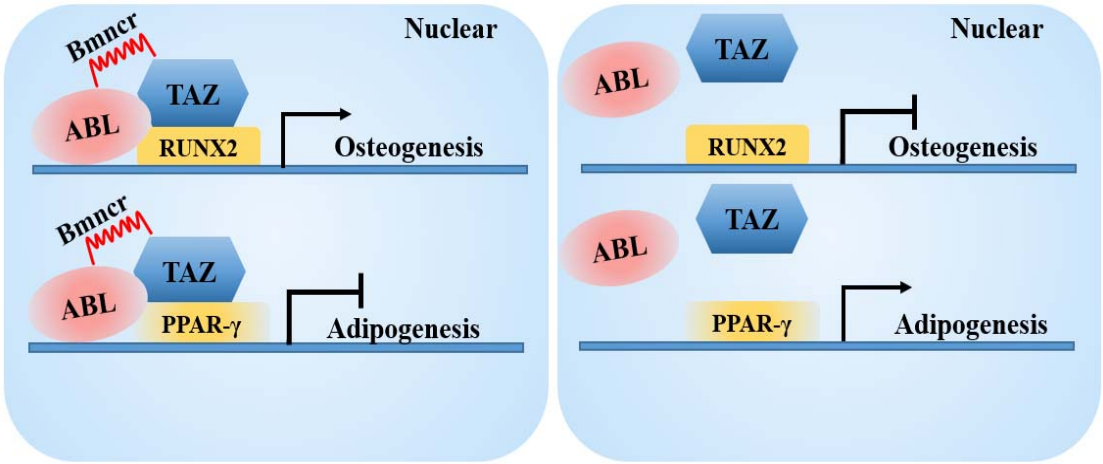

Figure S16. Schematic model of *Bmncr* as a scaffold for the TAZ and ABL complex.

Schematic model indicating *Bmncr* serves as a scaffold for the TAZ and ABL complex to promote the assembly of TAZ with RUNX2/PPARG, which enhances osteogenesis and inhibits adipogenesis.

Figure S17

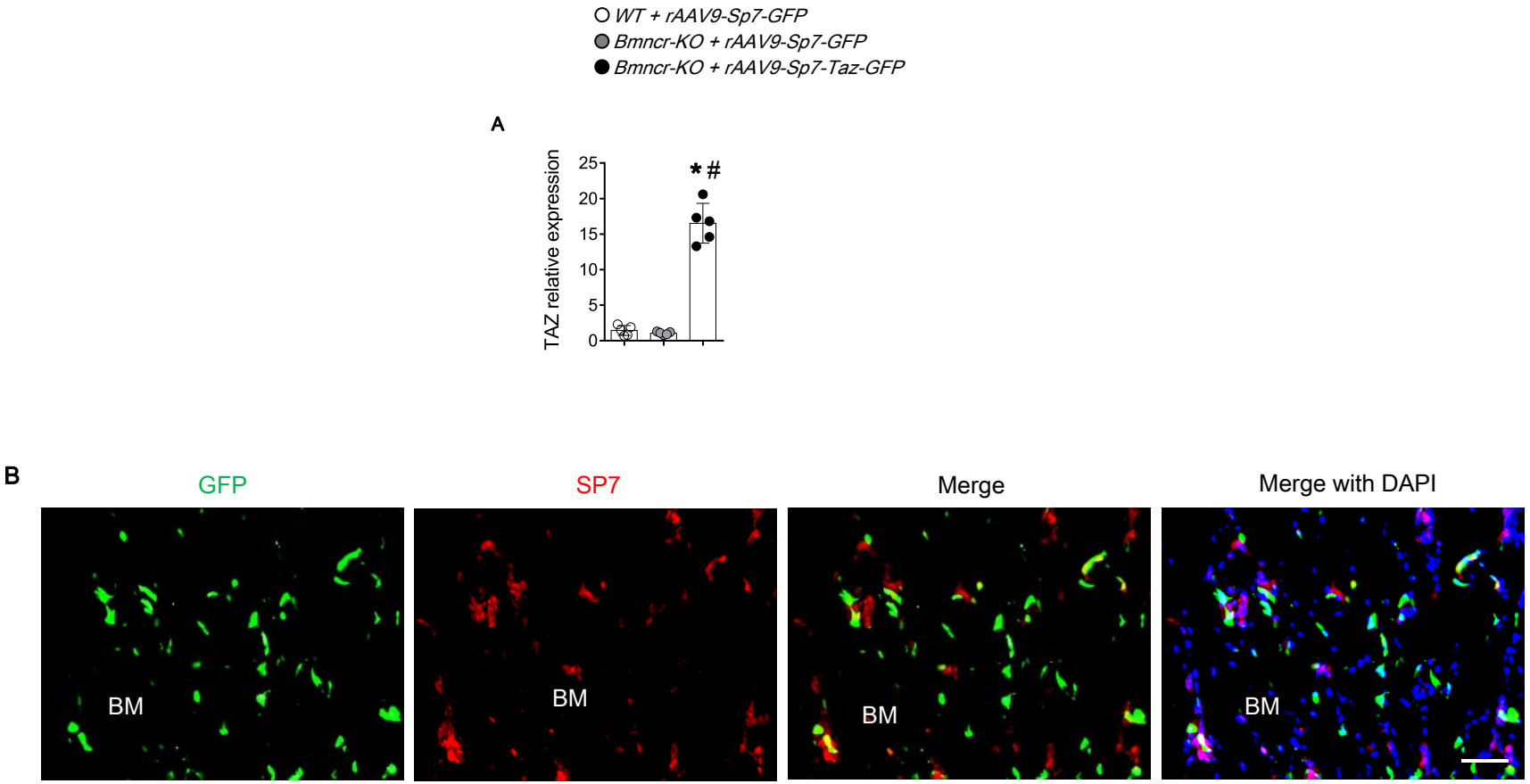

Figure S17. Validation of rAAV9-Sp7-Taz-GFP injection.

(A) *Taz* expression in $SP7^{+}$ osteoprogenitors in the mice infected with rAAV9-Sp7-Taz-GFP or control groups.

(**B**) Representative immunofluorescence staining images of GFP (green) with Sp7 (red) in femora from rAAV9-Sp7-Taz-GFP treated mice. Nuclei, DAPI (blue). Scale bar: 100 μM.

Figure S18

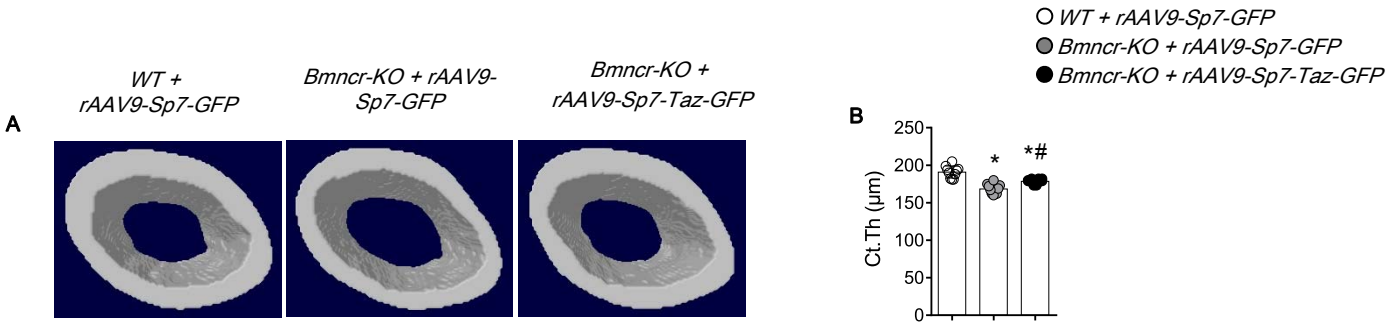

Figure S18. *Bmncr-KO mice with rAAV9-Sp7-Taz-GFP injections* showed increased cortical bone thickness in the femora compared to *WT* controls.

(**A-B**) μCT images (**A**) and quantitative μCT analysis (**B**) of cortical bone thickness in femora.

n = 10 per group. Data shown as mean ± s.d. *P < 0.05 versus WT+rAAV9-Sp7-GFP group; # P < 0.05 versus Bmncr-KO+rAAV9-Sp7-GFP group (one-way ANOVA).

Supplementary table 1. Nucleotide sequences of primers used for human cells quantitative RT-PCR detection

Primer	sequence (5' to 3')
BMNCR (human)	F: GGAGTCCAGAAGGCGGTAGT
	R: CTGAAAGTAGGTGCCGAGGA
PPARG (human)	F: ACCAAAGTGCAATCAAAGTGGA
	R: ATGAGGGAGTTGGAAGGCTCT
FABP4 (human)	F: ACTGGGCCAGGAATTTGACG
	R: CTCGTGGAAGTGACGCCTT
RUNX2 (human)	F: TGGTTACTGTCATGGCGGGTA
	R: TCTCAGATCGTTGAACCTTGCTA
BGLAP (human)	F: CACTCCTCGCCCTATTGGC
	R: CCCTCCTGCTTGGACACAAAG
ALP (human)	F: ACTGGTACTCAGACAACGAGAT
	R: ACGTCAATGTCCCTGATGTTATG

Note: F, forward primer; R, reverse primer.

Supplementary Table 2. Nucleotide sequences of primers used for mice cells quantitative RT-PCR detection

Primer	sequence (5' to 3')
Bmncr (mouse)	F: CTAAGCGAACTCGGGAGC
	R: CACAGCAGGATTGATGGATG
Fmod (mouse)	F: GGGGCAAGGACTGTTGGAGGAG
	R: CCAGGTCTGGAGCCAAGAACGTAGT
Pparg (mouse)	F: ATGGTTGACACAGAGATGC
	R: GAATGCGAGTGGTCTTCC
Fabp4 (mouse)	F: AAGGTGAAGAGCATCATAACCCT
	R: TCACGCCTTTCATAACACATTCC
Runx2 (mouse)	F: GAAATGCCTCCGCTGTTATG
	R: AGGTGAAACTCTTGCCTCGTC
Bglap (mouse)	F: AAGCAGGAGGGCAATAAGGT
	R: ATGCGTTTGTAGGCGGTCTT
Sp7 (mouse)	F: ATGGCGTCCTCTCTGCTTG
	R: TGAAAGGTCAGCGTATGGCTT
Alpl (mouse)	F: CCCCATGTGATGGCGTAT
	R: CGGTAGGGAGAGCACAGC

Note: F, forward primer; R, reverse primer.

Full unedited gel

Fig. 4D

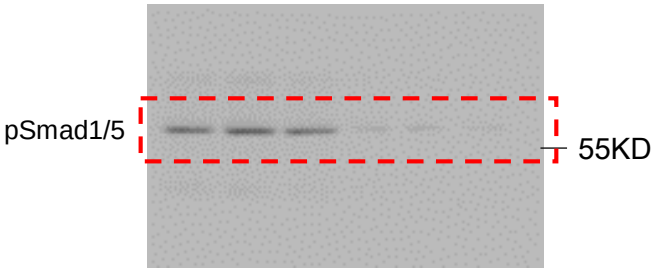

Fig. 4D

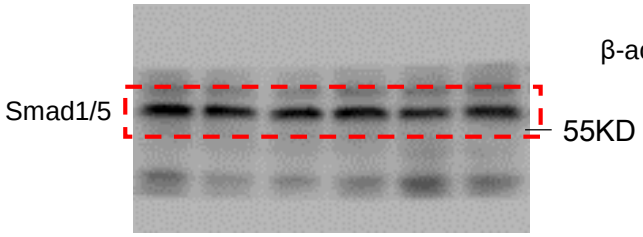

Fig. 4D

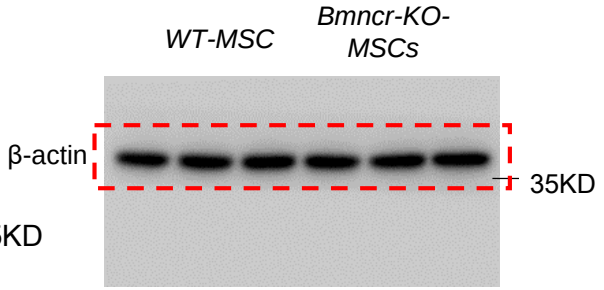

Fig. 5B

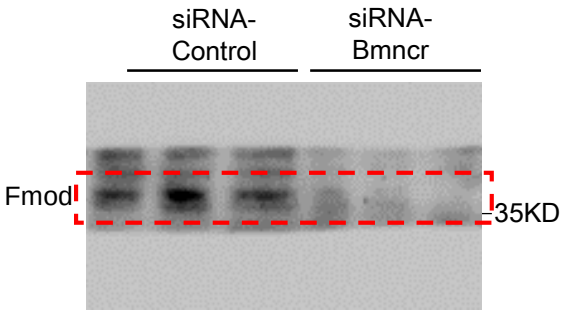

Fig. 5B

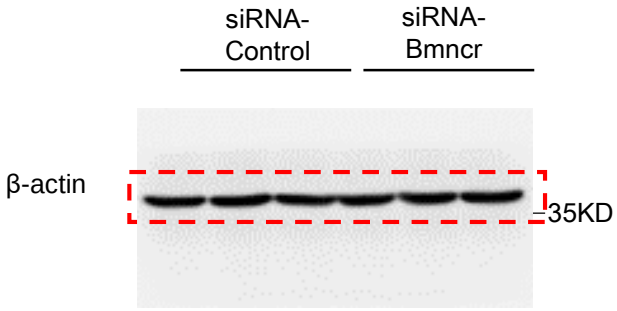

Full unedited gel

Fig. 7G

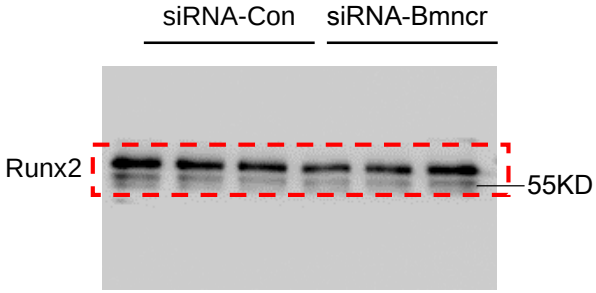

Fig. 7G

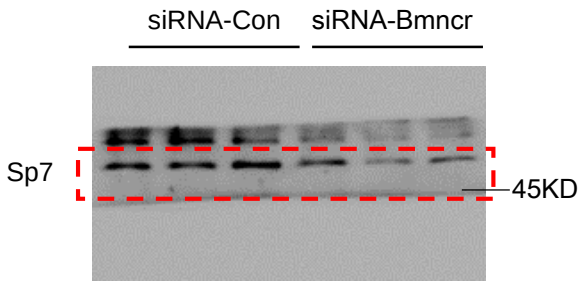

Fig. 7G

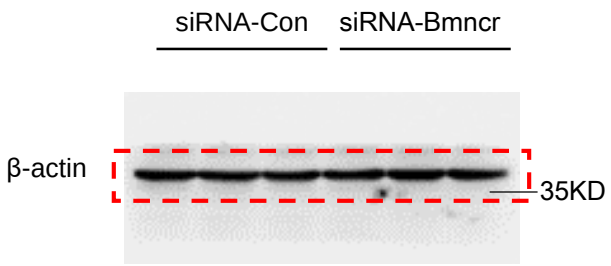

Fig. 7J

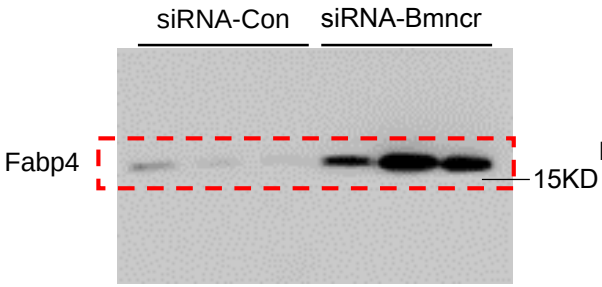

Fig. 7J

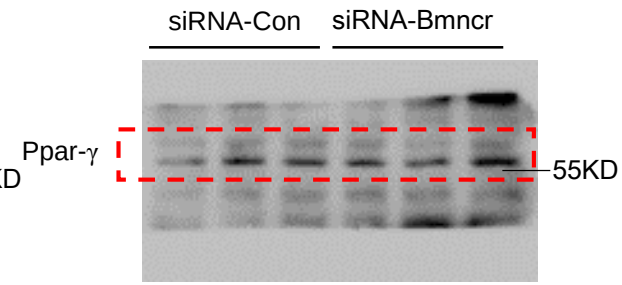

Fig. 7J

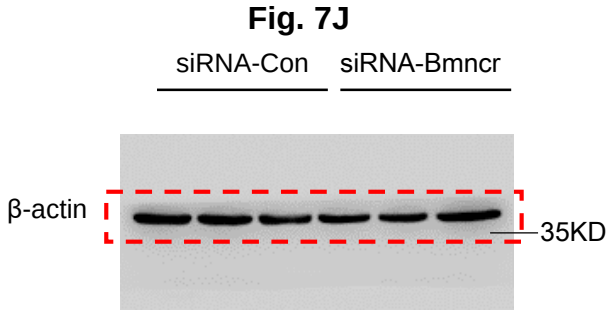

Full unedited gel

Fig. 8B

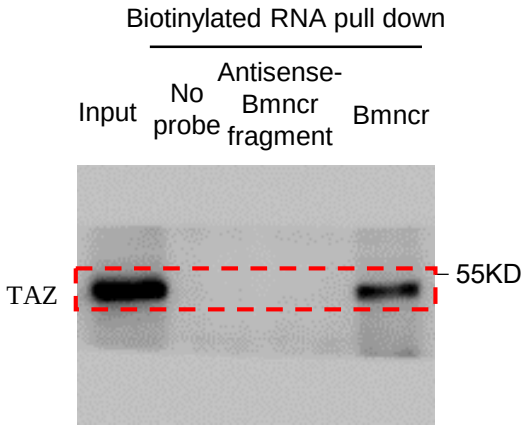

Fig. 8B

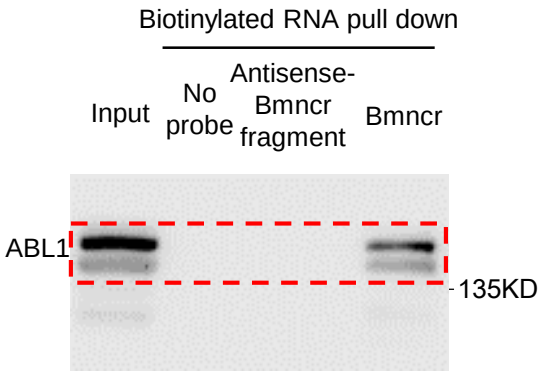

Fig. 8E

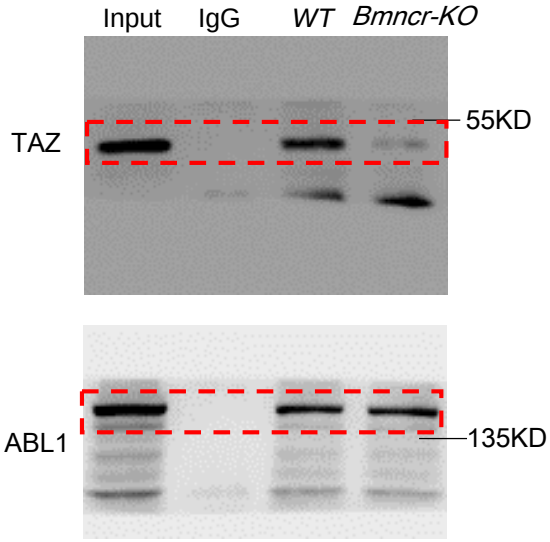

Fig. 8F

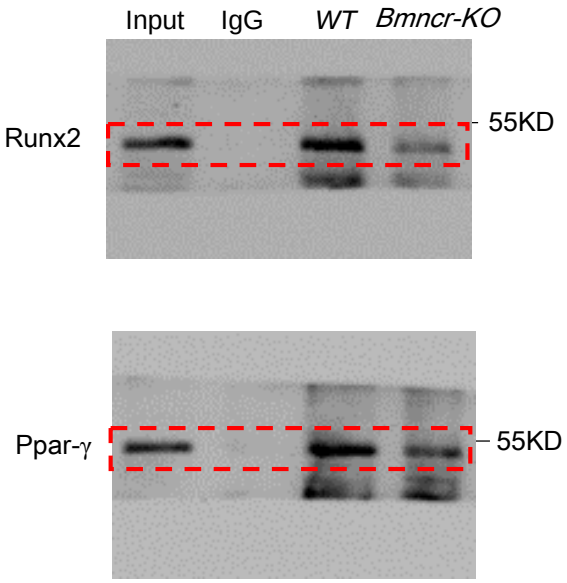

Full unedited gel

Fig. 8D

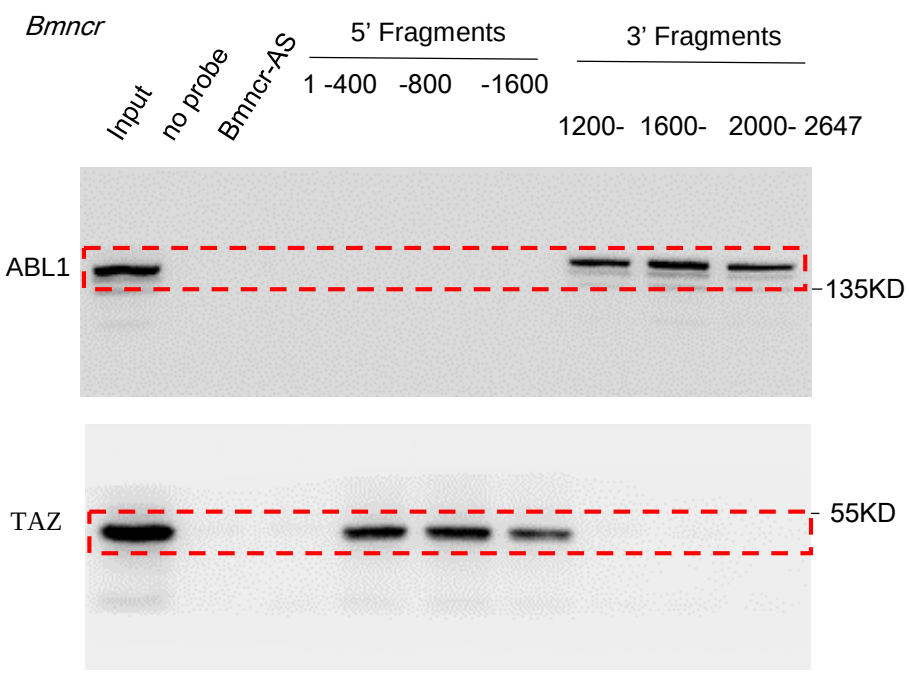

Fig. S8B

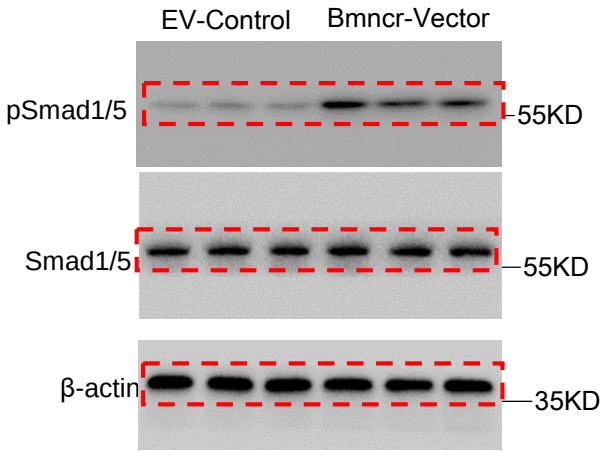

Fig. S9B

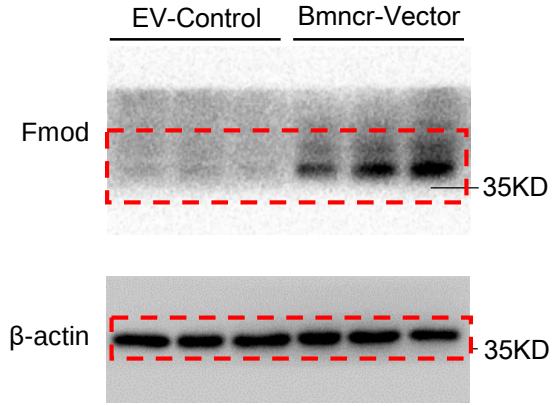

Full unedited gel

Fig. S15A